

# Surface Plasmon Resonance Thermodynamic and Kinetic Analysis as a Strategic Tool in Drug Design. Distinct Ways for Phosphopeptides to Plug into Src- and Grb2 SH2 Domains

Nico J. de Mol,<sup>\*,†</sup> Frank J. Dekker,<sup>†,‡</sup> Isabel Broutin,<sup>§</sup> Marcel J. E. Fischer,<sup>†</sup> and Rob M. J. Liskamp<sup>†</sup>

*Department of Medicinal Chemistry, Utrecht Institute for Pharmaceutical Sciences, Utrecht University, Sorbonnelaan 16, 3584 CA Utrecht, The Netherlands, and Laboratoire de Cristallographie et RMN Biologiques, UMR 8015 CNRS, Faculté de Pharmacie, Université René Descartes, 4 Avenue de l'Observatoire, 75270 Paris Cedex 06, France*

Received August 6, 2004

Thermodynamic and kinetic studies of biomolecular interactions give insight into specificity of molecular recognition processes and advance rational drug design. Binding of phosphotyrosine (pY)-containing peptides to Src- and Grb2-SH2 domains was investigated using a surface plasmon resonance (SPR)-based method. This SPR assay yielded thermodynamic binding constants in solution, and the kinetic information contained in the SPR signal allowed kinetic analysis, which demonstrated distinct ways for pY ligands to interact with the SH2 domains. The results for binding to Src SH2 were consistent with sequestration of water molecules in the interface of the pYEEI peptide/Src SH2 complex. The results for a pYVNV peptide binding to Grb2 SH2 suggested a conformational change for Grb2 SH2 upon binding, which is not observed for Src SH2. Binding of a cyclic construct, allowing the pYVNV sequence in the bound conformation, did not have the expected entropy advantage. The results suggest an alternative binding mode for this construct, with the hydrophobic ring-closing part interacting with the protein. In all cases, except for full-length Grb2 protein, the affinity for the immobilized peptide at the SPR sensor and in solution was identical. This study demonstrates that SPR thermodynamic and kinetic analysis is a useful strategic tool in drug design.

## Introduction

In cell signaling, complex cascades of protein–protein and protein–lipid interactions occur that eventually translate an extracellular stimulus through a receptor into well-defined cellular processes. Intracellular signaling proteins function as molecular switches, ultimately leading to aggregation of proteins into interacting networks or just recruiting components to a functional position. Protein phosphorylation is one of the tools to switch on signaling routes in the molecular information circuit.

In these cellular communication processes, not only binding and affinity are relevant but also allosteric changes. Kinetics and changes in protein dynamics are crucial for the functionality of the binding process. As a consequence, in drug design not only the affinity is important but also the kinetics and thermodynamics associated with the interaction may be decisive. Techniques such as structural analysis using X-ray crystallography<sup>1,2</sup> and NMR<sup>3,4</sup> have been of major importance for the enhancement of the structural basis of rational drug design. Newer techniques such as calorimetry,<sup>5,6</sup> protein mass spectrometry,<sup>7,8</sup> and surface plasmon resonance (SPR)<sup>9,10</sup> now have also found a place as strategic tools in protein-binding studies. SPR is especially interesting as it also offers kinetic information<sup>10,11</sup>

along with affinity data and can be used for thermodynamic studies,<sup>12,13</sup> although examples of this are still scarce.

Here, we report on thermodynamic and kinetic studies of phosphotyrosine (pY)-containing peptides binding to SH2 domains, using SPR assays at various temperatures. For this study, we choose two SH2 domains, Src and Grb2, for which there are firm structural bases for understanding ligand recognition. This allows a structural interpretation of the obtained thermodynamic and kinetic information.

Many signaling proteins contain one or two modular SH2 domains that are able to recognize specific peptide sequences containing phosphorylated tyrosine residues. Further specificity is determined by the two or three amino acids immediately C-terminal of the tyrosine.<sup>14</sup> In a number of proteins, specificity is potently increased by occurrence of SH2 domains in tandem, recognizing a biphenylphosphotyrosine motif, with proper spacing.<sup>15</sup> Phosphotyrosine ligand/SH2 domain interactions are widely studied, not in the least because the SH2 domains are interesting targets for therapeutic intervention and design of drugs against, among others, cancer, osteoporosis, and allergy.<sup>16,17</sup>

For binding to the Src family of SH2 domains, the parallel between functioning as a modular switch and electrical circuits in everyday life can be even drawn further as its binding mode with the consensus sequence pYEEI has been compared to a “two-pronged plug two-holed socket” and the phosphorylation state functions as an on–off switch.<sup>18</sup> The pYEEI peptide binds in an extended conformation (Figure 1a). The two holes form

\* Author to whom correspondence should be addressed. Phone: +31-30-2536989. Fax: +31-30-2536655. E-mail: n.j.demol@pharm.uu.nl.

† Utrecht University

‡ Present address: Department of Chemical Biology, Max Planck Institute for Molecular Physiology, Otto Hahn Strasse 11, 44227 Dortmund, Germany.

§ Université René Descartes

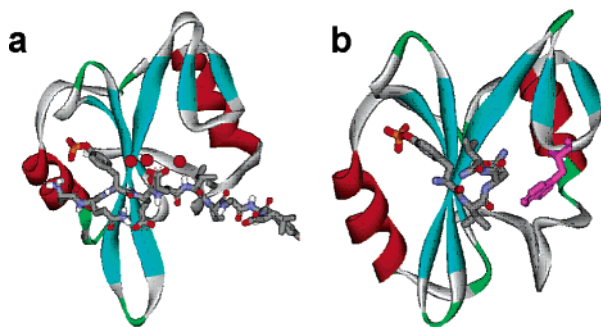


**Figure 1.** X-ray structures of Src- and Grb2 SH2 domains binding to phosphotyrosyl peptides. (a) Src SH2 binding to an 11-mer pYEEI peptide derived from hamster middle T antigen. Three water molecules in a hydrogen-bonding network around Glu(pY + 2) are indicated as red dots (PDB entry 1SPS). (b) Grb2 SH2 binding to KPFpYVNV-NH<sub>2</sub> (only pYVNV shown). Trp 121 is indicated in magenta (PDB entry 1TZE).

binding pockets for the pY and I residues, both glutamate residues lie along the surface and are almost completely accessible to solvent. Well-resolved water molecules may form a hydrogen-bonding network that links Glu(pY + 2) with the SH2 domain.<sup>19</sup> These water molecules are indicated in Figure 1a. Interestingly, this mode of binding can be completely changed by a single amino acid mutation, introducing a bulky tryptophan in the EF1 loop of the Src SH2 domain.<sup>20</sup> In the SH2 domains of Sem-5, drk, and Grb2, such a Trp residue occurs in the EF loop, and these domains selectively select pY-(L/V)-N-(V/P) sequences.<sup>20</sup> The crystal structure of the complex of Grb2 SH2 with a pYVNV peptide reveals that the peptide binds in a  $\beta$ -turn conformation (Figure 1b). Trp 121 closes the binding site C-terminal to the phosphotyrosyl residue of the ligand and prevents it from adopting the extended conformation as found in Src family SH2 domains.<sup>21</sup>

Next to the single Src- and Grb2 SH2 domains, in our study full-length Grb2 protein also was included. Full-length Grb2 consists of a central SH2 domain flanked by two flexible linked SH3 domains.<sup>22</sup>

Our aim is to explore the use of SPR in a combined thermodynamic and kinetic approach and to compare the results to those obtained from other techniques. Thermodynamic studies of ligands binding to SH2 domains using isothermal titration calorimetry (ITC) have been published before.<sup>18,23–25</sup> In general, the thermodynamic parameters derived from the SPR experiments compare well to those from ITC. Thermodynamic and kinetic information is found to be complementary to each other and is consistent with the contribution of a water network in the binding interface of Src SH2. At lower temperatures, SPR kinetic analysis indicates a conformational change upon binding to the Grb2 protein but not for Src SH2. The thermodynamics of binding of a designed cyclic construct of the pYVNV peptide, in which the pYVNV sequence can be “locked” in the binding  $\beta$ -turn conformation, suggests that this construct binds in an alternative mode in which the ring-closing part is involved in hydrophobic interactions with the protein.

## Results

### Thermodynamic Equilibrium Analysis of pYEEI Peptide Binding to the v-Src SH2 Domain.

In our

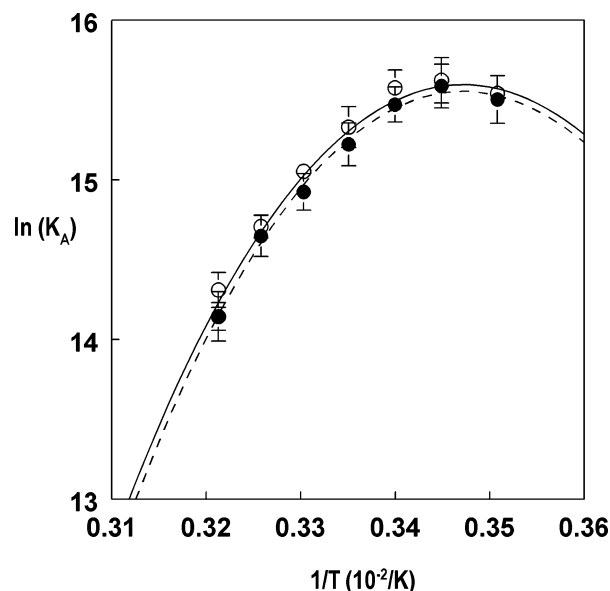


**Figure 2.** Van't Hoff plot for binding of peptide EPQpYEEIPIYL-NH<sub>2</sub> to the v-Src SH2 domain in HBS buffer pH 7.4. Direct binding at the SPR sensor surface ( $K_C$ ), solid line. Affinity in solution from SPR competition experiments ( $K_S$ ), dotted line. The bars indicate the standard error in the affinity data. The lines are the fits according to the integrated van't Hoff equation (eq 3).

**Table 1.** Thermodynamic Parameters for Binding of the EPQpYEEIPIYL-NH<sub>2</sub> Peptide to the v-Src SH2 Domain in HBS Buffer pH 7.4 at the Sensor Surface and in Solution, as Derived from the Van't Hoff Plots (Figure 2)

	sensor surface	solution
$\Delta H^\circ$ (kcal/mol) <sup>a</sup>	$-9.4 \pm 0.6$	$-9.6 \pm 0.3$
$T\Delta S^\circ$ (kcal/mol) <sup>a</sup>	$-0.3 \pm 0.6$	$-0.6 \pm 0.3$
$\Delta C_p$ (cal/mol/K)	$-920 \pm 160$	$-950 \pm 90$
$\Delta G^\circ$ (kcal/mol) <sup>a,b</sup>	$-9.1$	$-9.0$
$K_D$ (nM) <sup>a</sup>	$220 \pm 30$	$237 \pm 35$

<sup>a</sup> At reference temperature 25 °C. <sup>b</sup> Calculated from  $\Delta G^\circ = \Delta H^\circ - T\Delta S^\circ$ .

assay, two types of affinity data are collected: (1)  $K_C$  is the (apparent) binding constant for the interaction at the SPR sensor surface and is obtained from fitting the equilibrium SPR signal of binding protein in a concentration range to a one-site binding isotherm (Experimental Section), and (2)  $K_S$ , which is defined as the thermodynamic binding constant for bimolecular binding in solution, is derived from competition experiments with a constant protein concentration and the peptide under investigation in a concentration range, as previously described.<sup>26</sup>  $K_C$  as well as  $K_S$  has been assayed at temperatures in a range from 10 to 40 °C.  $K_C$  might be influenced by artifacts related to the carboxymethylated dextran surface of the SPR sensor. However,  $K_S$  is a thermodynamic binding constant for the interaction in solution, which in principle is independent from effects due to the sensor matrix.<sup>26</sup>

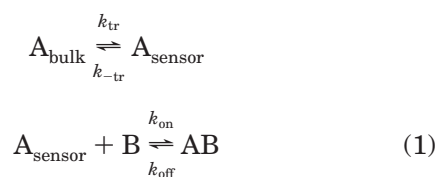
In Figure 2, the van't Hoff plots for  $K_C$  and  $K_S$  are shown, and the thermodynamic parameters derived from the van't Hoff plots (Experimental section) are given in Table 1. Interestingly, the plots for  $K_C$  and  $K_S$  are not significantly different, demonstrating that in this case the affinity at the sensor surface is identical to that in solution and that  $K_C$  is not influenced by the sensor environment. The curves are convex, indicating

a negative heat capacity ( $\Delta C_p$ ) value, and the binding is almost completely enthalpy driven at 25 °C.

Comparing the thermodynamic parameters with values from the literature as assayed with isothermal titration calorimetry (ITC), it appears that our  $\Delta H^\circ$  and  $T\Delta S^\circ$  values compare very well with those for an identical peptide binding to the Src SH2 domain.<sup>24</sup> However, reported  $\Delta C_p$  values derived from ITC, for binding of pYEEI peptides to the Src SH2 domain at pH 6.0 (approximately  $-200$  (cal/mol)/K), are considerably smaller than those observed by us.<sup>18,27</sup> The reason for this deviation in  $\Delta C_p$  is not clear.

**Kinetic Analysis of pYEEI Peptide Binding to the v-Src SH2 Domain.** The SPR signal upon binding as a function of time contains kinetic information, and this allows a full kinetic characterization of the binding with data from the same experiments as used for the equilibrium assays.

In Figure 3, sensorgrams for the association phase at various SH2 concentrations are shown for 15 and 40 °C. At 15 °C, the increase of the SPR signal is considerably slower than that at 40 °C. The kinetic information contained in the SPR curves can be analyzed according to a predefined binding model using the program CLAMP. Global analysis of the SPR curves from experiments with different protein concentrations with CLAMP yields the kinetic parameters as defined by the binding model.<sup>11</sup> We explored a simple binding model for a bimolecular interaction as described in eq 1.



In this model, A is the protein, and B is the immobilized peptide. This binding model also includes a transport step for diffusion of the SH2 domain from the bulk solution to the sensor surface. As reported previously, such a transport step has to be included because binding of SH2 domains to an immobilized peptide is strongly influenced by mass transport limitation (MTL).<sup>8,28</sup> At high association rates or high binding capacity, diffusion of the protein from the bulk to the sensor surface becomes rate-limiting. As shown in Figure 3, the SPR signal for binding to the Src SH2 domain can be well-described by this model.

In principle, the off-rate ( $k_{\text{off}}$ , eq 1) can be obtained from the dissociation phase of the sensorgrams. As reported previously, for MTL influenced processes the dissociation phase is strongly influenced by rebinding of released protein.<sup>28,29</sup> Rebinding is further enhanced by the cuvette design of the IBIS instrument, because released protein is not removed by a flow.<sup>28</sup> Therefore, separate experiments have been performed to assay  $k_{\text{off}}$ , by recording the decay of the SPR signal upon addition of substantial amounts of competing pYEEI peptide to prevent rebinding, as previously described.<sup>8</sup> Such dissociation experiments have been performed in the temperature range of 10–30 °C. At higher temperatures, the baseline was too much disturbed due to small temperature effects upon addition of the peptide.

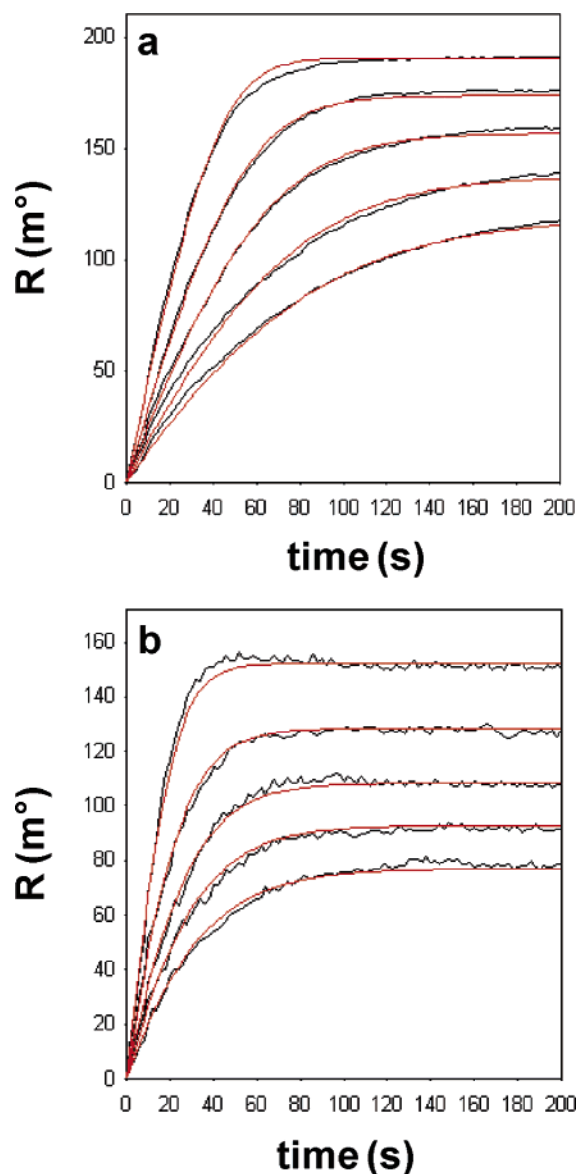


**Figure 3.** Sensorgrams of binding of the v-Src SH2 domain (concentration range 250–1000 nM) to immobilized EPQpY-EEIPIYL peptide at (a) 15 °C and at (b) 40 °C. The red curves are the fits to the experimental data according to the bimolecular MTL model (eq 1).

Dissociation proceeds extremely rapidly, and  $k_{\text{off}}$  is approximately  $1 \text{ s}^{-1}$ , as also observed for other SH2 domains.<sup>30,31</sup> On the basis of the association constant  $K_A$  and the off-rate, the association rate constant  $k_{\text{on}}$  (eq 1) was calculated ( $k_{\text{on}} = K_A k_{\text{off}}$ ). The temperature dependence of  $k_{\text{on}}$  and  $k_{\text{off}}$  allows analysis of the thermodynamics of activation to the binding transition state, based on the Eyring plots as shown in Figure 4.

It appears that the plot for  $k_{\text{off}}$  is linear and only slightly dependent on temperature, corresponding to a small activation enthalpy ( $\Delta H^\ddagger$ ) for dissociation. As a consequence, the plot for  $k_{\text{on}}$  has the convex curvature also observed in the van't Hoff plot. Here, we have an example of non-Arrhenius kinetics; it appears that  $k_{\text{on}}$  at a higher temperature is actually decreasing. These data are consistent with the argument of Truhlar and Kohen that if the Arrhenius (or Eyring) plot is convex, then the rate constant under certain conditions must actually decrease with increasing energy (Discussion).<sup>32</sup>

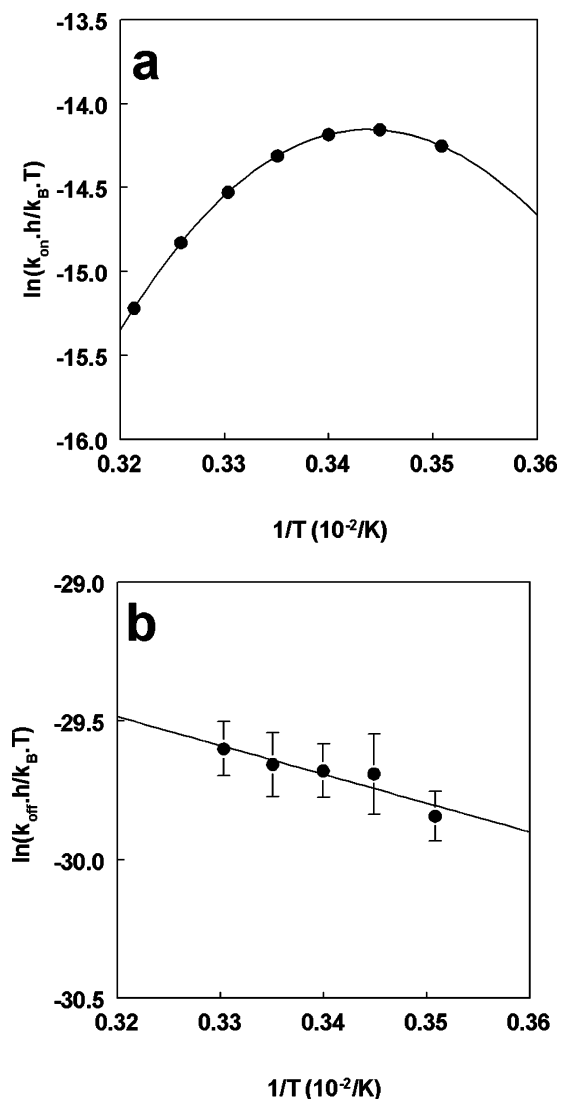


**Figure 4.** Eyring plots for (a)  $k_{\text{on}}$  and (b)  $k_{\text{off}}$  of the v-Src SH2 domain binding to immobilized EPQpYEEIPIYL peptide. The dissociation rate  $k_{\text{off}}$  has been assayed in the presence of 0.22 mM pYEEI peptide to prevent rebinding. The association rate is calculated from  $k_{\text{on}} = K_A k_{\text{off}}$ . The fit in panel a is according to eq 3 (Experimental Section).

**Table 2.** Parameters for Activation of the Transition State for Binding of EPQpYEEIPIYL-NH<sub>2</sub> to v-Src SH2 Domain<sup>a</sup>

activation parameter	association <sup>c</sup>	dissociation <sup>d</sup>
$\Delta H^\ddagger$ (kcal/mol) <sup>b</sup>	$-6.9 \pm 0.1$	$2.0 \pm 0.6$
$T\Delta S^\ddagger$ (kcal/mol) <sup>b</sup>	$-15.5 \pm 0.1$	$-15.5 \pm 0.6$
$\Delta C_p^\ddagger$ (cal/mol/K)	$940 \pm 10$	0
$\Delta G^\ddagger$ (kcal/mol) <sup>b,e</sup>	8.6	17.5

<sup>a</sup> The activation parameters  $\pm$  standard error are derived from fits of the Eyring plots in Figure 4. <sup>b</sup> At reference temperature 25 °C. <sup>c</sup> Calculated from eq 3. <sup>d</sup> Calculated from eq 4. <sup>e</sup> Calculated from  $\Delta G = \Delta H - T\Delta S$ .

The activation parameters for formation and dissociation of the transition state have been obtained from fitting the data in Figure 4 to eqs 3 and 4 (Experimental Section). The derived thermodynamic parameters for activation are shown in Table 2.

The formation of the transition state for binding of the Src SH2 domain to the pYEEI peptide is characterized by a considerable decrease in entropy and a favorable enthalpy. The decrease in entropy indicates

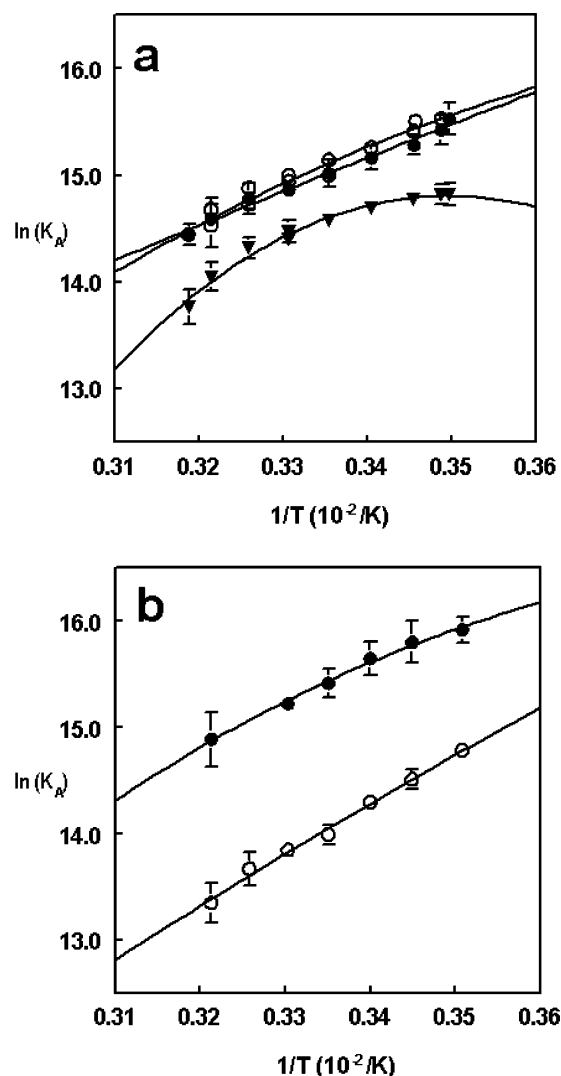


**Figure 5.** Van't Hoff plots for binding of pYVNV peptides to (a) the Grb2 SH2 domain and (b) full-length Grb2 in HBS buffer pH 7.4. Affinity at the sensor surface ( $K_C$ ) binding to immobilized PSpYVNVQN-NH<sub>2</sub> (○) and affinity in solution ( $K_S$ ) from SPR competition experiments with PSpYVNVQN-NH<sub>2</sub> (●) and cyclic pYVNV peptide (▼) are shown.

that formation of the transition state is accompanied by structural ordering.

**Thermodynamic Equilibrium Analysis of pYVNV Peptides Binding to the Grb2 SH2 Domain and Full-Length Grb2 Protein.** In a similar way as described above for the Src SH2 domain, a van't Hoff thermodynamic analysis was performed for binding of a pYVNV peptide to the Grb2 SH2 domain and the full-length Grb2 adaptor. The van't Hoff plots are shown in Figure 5.

We also included a cyclic peptide (Chart 1). As previously reported, molecular modeling showed that the pYVNV binding epitope in this construct can adopt a low-energy conformation that closely resembles the  $\beta$ -turn of the noncyclic analogue binding to Grb2 SH2.<sup>33</sup> It was expected that binding of such a cyclic construct has an entropy advantage.

Comparing the van't Hoff plots for Grb2 SH2 to those for Src SH2, it is striking that now the curves are practically linear, except that of the cyclic construct. For binding to the single SH2 protein, again no significant difference between the affinity in solution and at the

**Table 3.** Thermodynamic Parameters for Binding of pYVNV Peptides to a Single Grb2 SH2 Domain and Full-Length Grb2 in HBS Buffer pH 7.4<sup>a</sup>

	single Grb2 SH2			full-length Grb2	
	sensor surface	solution	solution cyclic pYVNV	sensor surface	solution
$\Delta H^\circ$ (kcal/mol) <sup>b</sup>	-6.8 ± 0.4	-6.3 ± 0.3	-5.6 ± 0.3	-9.4 ± 0.4	-7.3 ± 0.3
$T\Delta S^\circ$ (kcal/mol) <sup>b</sup>	2.2 ± 0.4	2.6 ± 0.3	3.0 ± 0.3	-1.0 ± 0.4	1.9 ± 0.3
$\Delta C_p$ (cal/mol/K)	-100 ± 95	-10 ± 80	-460 ± 70	-35 ± 100	-140 ± 80
$\Delta G^\circ$ (kcal/mol) <sup>b,c</sup>	-9.0	-8.9	-8.6	-8.4	-9.2
$K_D$ (nM) <sup>b</sup>	270 ± 20	340 ± 40	450 ± 50	790 ± 60	200 ± 30

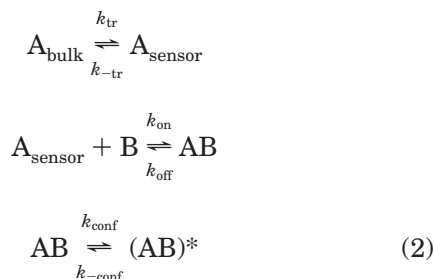
<sup>a</sup> Parameters derived from van't Hoff plots shown in Figure 5. <sup>b</sup> At reference temperature 25 °C. <sup>c</sup> Calculated from  $\Delta G^\circ = \Delta H^\circ - T\Delta S^\circ$ .

sensor matrix is obtained. However, for full-length Grb2 the affinity in solution is approximately 3- to 4-fold higher than that at the sensor matrix.

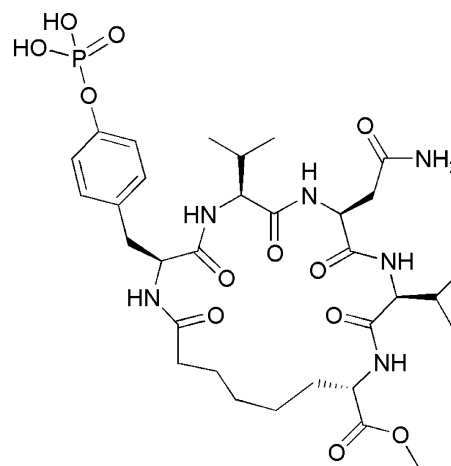
The thermodynamic parameters for binding to the Grb2 proteins derived from the van't Hoff plots are included in Table 3. The binding of linear pYVNV peptide is enthalpy driven also with an entropic contribution. This is found for the single SH2 domain as well as the full-length protein. The results from the SPR thermodynamic analysis, including the  $\Delta C_p$  value, compare well with published results from ITC experiments with a somewhat shorter pYVNV peptide binding to Grb2 SH2.<sup>25</sup> Comparing the solution affinities, it appears that the affinity of the full-length protein is somewhat higher than that of the single SH2 domain. This is due to a more favorable enthalpy contribution of approximately 1 kcal/mol, which is compensated by a slightly less favorable entropy contribution. The cyclic pYVNV construct has a convex van't Hoff plot, and a large negative  $\Delta C_p$  is found. At 25 °C, the cyclic construct has a slightly reduced affinity compared to the linear peptide, and the enthalpy and entropy at 25 °C are very similar (Table 3).

Only for the full-length Grb2 protein, the affinity in solution is found to be deviant from that at the sensor surface. This difference is caused by a higher entropy cost of approximately 3 kcal/mol for binding to the sensor, which is partly compensated for by the enthalpy.

**Kinetic Analysis of pYVNV Peptides Binding to the Grb2 SH2 Domain and Full-Length Grb2 Protein.** In Figure 6, sensorgrams for the full-length Grb2 protein binding to immobilized pYVNV peptide at 10 and 35 °C are shown. At 10 °C, the transport bimolecular model (eq 1) does not fit the experimental data well (Figure 6a). Binding to the Grb2 SH2 domain is accompanied by changes in dynamics and structure.<sup>8</sup> As shown in Figure 6b, a much better fit is obtained when a step is added representing a conformational change in the initial complex AB, leading to formation of the complex (AB)\* (eq 2).



The conformation change model better describes the biphasic nature of the curves for the Grb2 protein; the

**Chart 1.** Cyclic Construct of the pYVNV Peptide

initial rapid increase of the signal is followed by a slower increase before reaching equilibrium. At 35 °C, equilibrium is reached within a few seconds (Figure 6c), and the conformation model no longer gives a better fit than the bimolecular model of eq 1. For the single Grb2 SH2 domain, similar results were found (results not shown).

In the conformation change model, binding becomes more tight after the conformational change; therefore the association time might influence the value of  $k_{off}$ . As described for the Src SH2 domain above, at 15 °C  $k_{off}$  was assayed for the Grb2 protein by adding the pYVNV peptide after various association intervals (Figure 7).

Indeed, a slight difference in dissociation kinetics is observed; from three independent experiments,  $k_{off}$  was found to be  $0.90 \pm 0.15 \text{ s}^{-1}$  after short association (approximately 50 s), while upon reaching equilibrium the value of  $k_{off}$  was  $0.60 \pm 0.10 \text{ s}^{-1}$ . This finding supports the conformation change model.

For the Grb2 proteins,  $k_{on}$  and  $k_{off}$  have been determined at different temperatures. As reported, dissociation of the Grb2 SH2 domain was too fast to allow accurate measurements.<sup>8</sup> Even at low temperatures, no reliable assay was possible. The dissociation from the full-length protein was slower, and dissociation experiments have been performed from 10 to 30 °C. At 25 °C,  $k_{off}$  was found to be  $1.6 \pm 0.2 \text{ s}^{-1}$ , which is somewhat higher than the reported value for dissociation of a pYINQ peptide ( $0.2 \text{ s}^{-1}$ ) derived in a similar way.<sup>34</sup> Such high on- and off-rates are characteristic for SH2 domains. It should be noted that if the conformation change model applies (eq 2), then  $k_{on}$  and  $k_{off}$  formally are apparent rate constants and the apparent binding constant is composed of contributions from the initial binding step and the conformational equilibrium.<sup>8</sup>

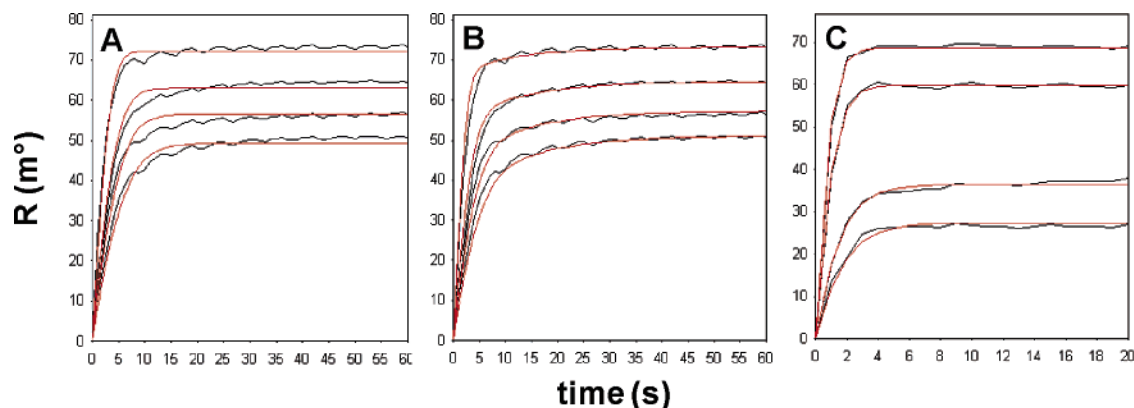


**Figure 6.** Global kinetic analysis of sensorgrams for binding of full-length Grb2 protein to immobilized PSpYVNVQN-NH<sub>2</sub> peptide. Experiments at 10 and 35 °C were performed with protein concentrations of 375–1000 and 500–2500 nM, respectively. The red curves are the global fits with the indicated binding models. (a) At 10 °C, fit with the transport bimolecular model (eq 1). (b) At 10 °C, fit with the conformation change model (eq 2). (c) At 35 °C, fit with the transport bimolecular model (eq 1).

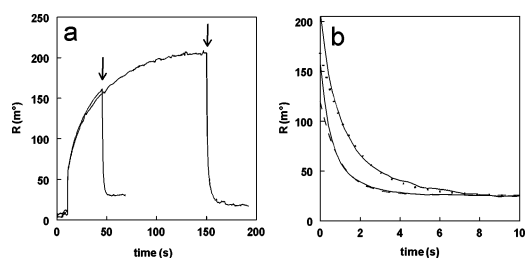


**Figure 7.** Effect of association time on dissociation of Grb2 protein from immobilized PSpYVNVQN-NH<sub>2</sub> peptide. During association of 1  $\mu$ M of Grb2 protein, PSpYVNVQN-NH<sub>2</sub> peptide was added at different time intervals (final concentration 0.22  $\mu$ M). (a) Sensorgrams, the arrows indicate the addition of peptide. (b) Overlay of the dissociation phase, fits according to eq 5. Short association, broken line; association to equilibrium, dotted line. The data for the first second were discarded from the fit due to bulk effects.

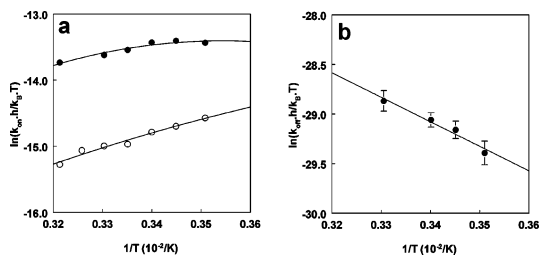


**Figure 8.** Eyring plots for (a)  $k_{on}$  and (b)  $k_{off}$  of full-length Grb2 protein binding to PSpYVNVQN-NH<sub>2</sub> peptide.  $k_{on}$  has been derived for binding in solution (●) and for binding to immobilized peptide at the sensor surface (○). The dissociation rate has been assayed from SPR competition experiments; it is assumed that this rate is equal for dissociation in solution and from the sensor surface. The association rate is calculated from  $k_{on} = K_A k_{off}$ . The  $k_{on}$  fits were performed with eq 3. For  $k_{off}$ , a linear fit was performed according to eq 4.

The Eyring plots for association and dissociation are shown in Figure 8. It is also found that binding to the Grb2 protein has non-Arrhenius kinetics;  $k_{on}$  decreases at higher temperature. However, compared to the Src SH2 domain, the variation of  $k_{on}$  with temperature is small (compare Figures 4a and 8a). The activation parameters for the transition state as derived from the Eyring plots are included in Table 4.

Formation of the transition state has unfavorable entropy and favorable enthalpy. It appears that formation of the transition state at the sensor surface has a higher entropy cost than that formed in solution of

**Table 4.** Parameters for Activation to the Transition State of pSpYVNVQN-NH<sub>2</sub> Binding to Full-Length Grb2 Protein in Solution and at the Sensor to Immobilized Peptide<sup>a</sup>

activation parameter	association <sup>c</sup> sensor	association <sup>c</sup> solution	dissociation <sup>d</sup>
$\Delta H^\ddagger$ (kcal/mol) <sup>b</sup>	$-4.5 \pm 0.4$	$-2.3 \pm 0.3$	$4.9 \pm 0.7$
$T\Delta S^\ddagger$ (kcal/mol) <sup>b</sup>	$-13.3 \pm 0.4$	$-10.3 \pm 0.3$	$-12.2 \pm 0.7$
$\Delta C_p^\ddagger$ (cal/mol/K)	$-45 \pm 100$	$-150 \pm 80$	0
$\Delta G^\ddagger$ (kcal/mol) <sup>b,e</sup>	8.8	8.0	17.1

<sup>a</sup> Activation parameters  $\pm$  standard errors are derived from fits of the Eyring plots in Figure 8. <sup>b</sup> At reference temperature 25 °C. <sup>c</sup> Calculated from eq 3. <sup>d</sup> Calculated from eq 4. <sup>e</sup> Calculated from  $\Delta G = \Delta H - T\Delta S$ .

approximately 3 kcal/mol, which is compensated by a higher enthalpy gain of approximately 2 kcal/mol (Table 4).

## Discussion

The thermodynamic data derived from the SPR experiments compare well to literature data originating from ITC experiments. The only exception is the large negative value for the heat capacity  $\Delta C_p$  of almost  $-1000$  (cal/mol)/K that we observe. From ITC assays using similar peptides, much smaller negative values for  $\Delta C_p$  of around  $-200$  (cal/mol)/K are reported.<sup>18,27</sup> The reason for this large difference in  $\Delta C_p$  value is not clear; at 25 °C, the values for  $\Delta H^\circ$  and  $\Delta S^\circ$  conform to the results from ITC for binding of an identical peptide.<sup>24</sup> As discussed below, a large negative  $\Delta C_p$  agrees with structural considerations. For the linear pYVNV peptide binding to Grb2 proteins, the observed  $\Delta C_p$  value (Table 3) is close to the reported value of  $-145$  (cal/mol)/K.<sup>25</sup> These findings give confidence in the parameters derived from our SPR experiments.

The energy transitions in the binding process for Src SH2 and full-length Grb2 are schematically represented in Figure 9. The free energy changes are remarkably similar for both proteins. Furthermore, both proteins have a negative  $\Delta H^\circ$  for formation of the transition state and a negative entropy contribution to the free energy. However, the extent of the underlying enthalpy and entropy contributions is quite different. Furthermore, large differences in  $\Delta C_p$  value are observed. Association to Src SH2 proceeds with an outspoken convex curve, which is also found for the cyclic Grb2 SH2 ligand and indicates a large negative  $\Delta C_p$  value.

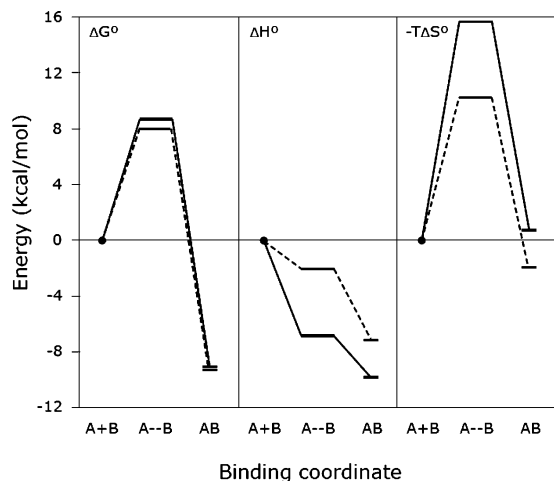


**Figure 9.** Energy transitions at 25 °C as function of the binding coordinate for binding of the pYEEI peptide to Src SH2 (solid lines) and pYVNV peptide to full-length Grb2 protein (dotted lines). A- B represents the transition state, data from Tables 2 and 4

All of the above-mentioned observations indicate important differences in the binding mode for Src- and Grb2 SH2. Here, the thermodynamic and kinetic observations will be discussed and interpreted in view of general observations with respect to thermodynamics of protein binding and the available structure information on these SH2 domains in particular.

Truhlar and Kohen<sup>32</sup> state that a convex Arrhenius (or Eyring) plot should be consistent with rate constants decreasing with temperature rise. Such types of kinetics are frequently found for protein folding. The Eyring plots indeed show non-Arrhenius association kinetics, with  $k_{on}$  rates being slower at higher temperatures (Figures 4 and 8). In general, a reasonable explanation for this is that at higher temperatures a wider region of conformational space is visited and that the probability of a flexible ligand having the right conformation for folding or binding is decreasing at higher temperature. This might especially hold for the pYVNV peptide, which binds in a specific  $\beta$ -turn fold to the Grb2 SH2 domain.

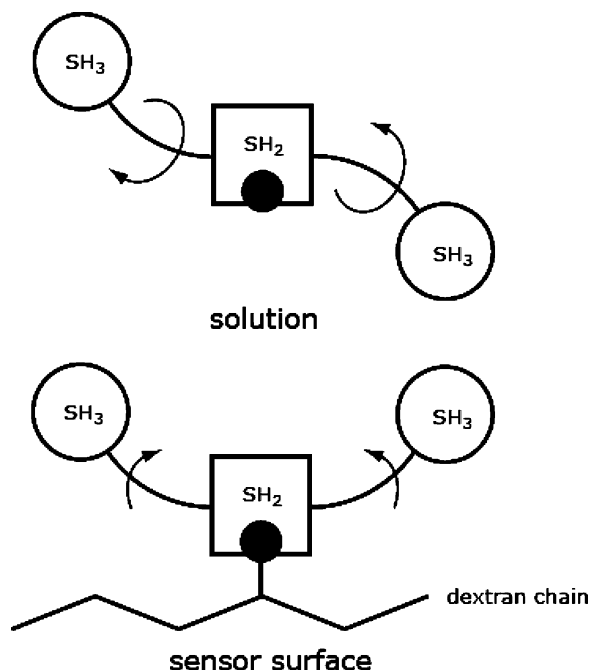
For the Src SH2 domain, the reason for the decrease of  $k_{on}$  with temperature is less obvious at first sight. The entropy cost for activation of the transition state for Src SH2 is 5 kcal/mol higher than that for Grb2 protein in solution, while the entropic contribution to the free binding energy is approximately 2 kcal/mol less (Figure 9). Therefore, formation of the transition state and binding is accompanied with more ordering than in the case of the Grb2 proteins. It has been demonstrated for Src SH2 as well as the Grb2 proteins that binding decreases the dynamics of the proteins. From hydrogen/deuterium exchange experiments, it appears that approximately 10 protons are less exchanged for these proteins upon binding.<sup>8,35</sup> Therefore, these changes in dynamics are expected to have a similar entropy price for Src- and Grb2 SH2 and do not explain the higher entropy cost for formation of the transition state and binding to Src SH2. A special role in binding affinity and selectivity to Src family SH2 domains has been attributed to interfacial water molecules in the complex. Especially, the pY + 2 glutamate residue is involved in binding to a network of water molecules (Figure 1a) that

probably also has a role in supporting the binding pocket of the pY + 3 residue.<sup>6</sup> Such a role for water molecules does not apply for binding to Grb2 SH2, where the pY + 2 asparagine forms a hydrogen bond network directly with the protein.<sup>36</sup> The organization of water in a network is reflected in the higher entropy cost of formation of the transition state and binding to Src SH2.

Frequently, values of  $\Delta C_p$  have been calculated based on empirical parametrization of the changes in polar and apolar solvent accessible surface area.<sup>37</sup> For binding of a pYEEI peptide to Src SH2, the predicted value of  $\Delta C_p$  based on calculated solvent accessible surface areas was found by Bradshaw et al. to be identical to their experimental value of approximately  $-200$  (cal/mol)/K, although in these calculations water molecules were not included.<sup>18</sup> Also, for a pYVNV peptide binding in an extended conformation to the Grb2 SH2 domain, the calculated  $\Delta C_p$  value was reported to be in agreement with the experimental value.<sup>25</sup> However, about the same time it appeared that this binding model is not correct and that the phosphopeptide binds in a  $\beta$ -turn conformation to Grb2 SH2.<sup>21</sup> Although such calculations with solvent accessible surface areas have been successful in some cases, effects of solvation and incorporation or release of water molecules during the binding process cause problems in the calculation of the solvent accessible surface. Sequestration of water molecules in the binding interface in general reduces the heat capacity when ligands bind to proteins. In an elegant model study, for a one point protein mutation leading to one additional, ordered water molecule upon binding, it has been found that  $\Delta C_p$  decreases approximately 150 (cal/mol)/K.<sup>38</sup> This leads to the conclusion that the large negative  $\Delta C_p$  value as derived from our SPR experiments is consistent with the organization of water molecules in a network in the Src SH2/peptide interface. The Src SH2 domain represents a highly promiscuous binding site. Henriques and Ladbury<sup>6</sup> have pointed out the role of this water network in the failure to design Src SH2 ligands with higher affinity than the natural ligands.

In previous studies using GST fusion proteins, a higher affinity at the sensor surface was found compared to the affinity in solution. This is explained by the avidity effect of GST dimers binding to the sensor surface.<sup>26</sup> In the present study for binding of the non-GST fusion Grb2 and v-Src SH2 domains, equal affinities in solution and at the sensor are observed (Figures 2 and 5a), as is expected when no additional interference with the sensor matrix occurs. Only for the full-length Grb2 protein, a lower affinity for the immobilized peptide is observed (Figure 5b). The affinity for the immobilized peptide is 3-fold lower than that of the single SH2 domain binding to the sensor surface, while in solution the affinity of SH2 and full-length protein is almost equal (Table 3). This last finding is in line with the structure of full-length Grb2 protein, with the SH3 domains linked opposite of the binding site of the SH2 domain, leaving it fully accessible.<sup>39</sup> Then, the question arises: what causes the exceptional, lower affinity of the full-length protein for the peptide coupled to the sensor surface? A possible explanation is that due to less partition of the larger full-length protein into the sensor matrix the local concentration of the protein is

**Scheme 1.** Limited Conformational Space Available for Full-Length Grb2 Protein When Bound to the Sensor Surface.



less, leading to a lower apparent affinity. However, through the use of the partition function presented by Schuck,<sup>29</sup> the partition coefficient for the dextran layer was calculated as 0.68 and 0.58 for the SH2 domain and full-length Grb2, respectively. This difference is too small to explain the 3-fold decreased affinity for the immobilized peptide. The activation parameters for the transition state indicate that binding to the immobilized peptide has a higher entropy cost than binding in solution. This is partly compensated by a more favorable enthalpy (Table 4), also the equilibrium parameters indicate a higher entropy price for binding to the sensor (Table 3). The full-length Grb2 protein is extremely flexible, and solution structures derived from molecular dynamics reveal that the two SH3 domains take different positions and orientations relative to the central SH2 domain, occupying an extended conformational space.<sup>22</sup> Therefore, a likely explanation for the diminished affinity of the peptide coupled to the sensor is restricted conformational freedom of the full-length protein due to limited space provided by the dextran matrix (Scheme 1). Such explanation is in accordance with the thermodynamic results.

For the Src SH2 domain, over the whole temperature range from 10 to 40 °C, binding can be described by a transport limited bimolecular binding model (Figure 3); this is in agreement with the fact that for this protein no major structural change upon binding has been observed.<sup>19</sup> The SPR curves for binding to the Grb2 SH2 domain and full-length Grb2 at lower temperatures are better described by a model including a conformational change (Figure 6). However, one must be careful to draw conclusions from kinetic analysis alone. The validity of the conformation model is supported by the decreased dissociation kinetics upon longer association (Figure 7). Furthermore, structural differences are found between the bound and the free protein<sup>36</sup> as well as changes in the protein dynamics upon binding as previously de-

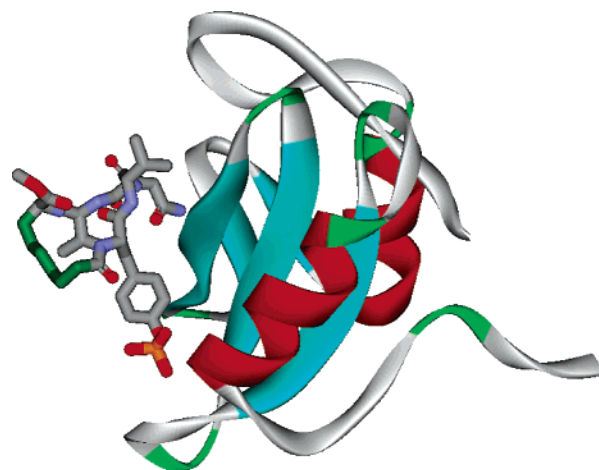


**Figure 10.** Model of the complex of the cyclic construct of the pYVNV peptide with the Grb2 SH2 domain. The construct has been superimposed on the linear pYVNV ligand, and the energy has been minimized, leaving the SH2 structure (PDB entry 1TZE) unchanged.<sup>33</sup> The pentamethylene bridge is indicated as green sticks.

scribed by us.<sup>8</sup> At temperatures higher than 30 °C, a bimolecular model is also sufficient (Figure 6). Apparently, at higher temperatures the conformation change is no longer separately resolvable.

As the phosphotyrosine ligand for Grb2 SH2 binds in a  $\beta$ -turn conformation, we and others have tried to fix this conformation in cyclic ligands.<sup>33,40,41</sup> From molecular modeling, it appeared that our cyclic compound (Chart 1) was able to adopt a similar  $\beta$ -turn conformation as the bound linear ligand. However, the assumed favorable entropy due to preorganization in the bound conformation did not result in increased affinity.<sup>33</sup> Here, the thermodynamic analysis indicates that the entropic contribution to binding is not significantly different from the linear peptide and that the enthalpy is somewhat more unfavorable (Table 3). A remarkable difference with the linear peptide is the more convex van't Hoff plot and the accompanying more negative  $\Delta C_p$  (Figure 5a, Table 3). A more negative  $\Delta C_p$  is compatible with increased burial of apolar surface upon binding;<sup>37</sup> this could involve the pentamethylene bridge in the cyclic compound.

A model of the cyclic construct, energy minimized in the Grb2 SH2 protein,<sup>33</sup> is shown in Figure 10. It appears that the pentamethylene bridge points to the solvent, without interactions with the protein. The more negative  $\Delta C_p$  suggests an alternative binding mode for the cyclic construct, involving the hydrophobic bridge. The binding site of the Grb2 SH2 domain is known to accommodate large hydrophobic moieties, especially at pY + 1.<sup>42</sup> It is interesting to note that cyclic pYVNV derived constructs with closing bridges having more polar functionality indeed have higher affinity than the linear peptide.<sup>40</sup>

## Conclusion

Most frequently SPR is used to assay affinity data. Our research presented here and that of others<sup>12,13</sup> demonstrates that reliable thermodynamic data can be derived from SPR experiments. It has been raised as a point of concern for thermodynamic studies using SPR that the affinity for an immobilized ligand at the sensor



surface may deviate from that in solution.<sup>43</sup> However, from SPR competition experiments, thermodynamic binding constants for the interaction in solution can be obtained.<sup>26</sup> The results of the present study indicate that in many cases the affinity in solution is identical to that at the sensor. Exceptions can be expected with very large proteins, where partition in the dextran layer is low,<sup>29</sup> and with very flexible proteins as illustrated here with full-length Grb2 protein. Use of SPR for thermodynamic studies has some attractive features. In general, much less material is needed than for calorimetry, with a much lower sample concentration, up to a 1000-fold less of the binding components. The much lower sample concentration may preclude artifacts due to, for example, protein aggregation. Notwithstanding this, direct measurement of enthalpy in a well designed experiment by calorimetry is a valuable tool.

Another important advantage of the SPR approach is the kinetic information that is obtained. The kinetic information allows transition state analysis and analysis of the binding mode by global analysis of the SPR curves. Our study demonstrates that thermodynamic and kinetic analysis using SPR can be positioned as a strategic tool in drug design, complementary to other techniques that give structural information such as X-ray crystallography, NMR, and protein mass spectrometry. Insight into the fundamentals of binding processes that goes beyond only the assessment of affinity, however important this is, is a driving force in the drug design process.

## Experimental Section

**Proteins.** The v-Src SH2 domain was a generous gift from Dr. John Ladbury, University College London. The protein contained 106 amino acids, which correspond to residues 144–249 of the Src protein.<sup>24</sup> The concentration of the protein was determined by micro-BCA assay (Bio-Rad). The mass of the protein (12.3 kDa) as obtained from ESI-MS is in excellent agreement with that determined by Chung et al.<sup>24</sup>

The Grb2 SH2 domain was expressed and purified as described previously.<sup>8</sup> Experiments with the SH2 domain were performed with the monomeric form.

The full-length Grb2 protein was expressed and purified as described by Guilloteau et al.<sup>44</sup> This protein was in the monomeric form.

**Peptide Synthesis.** The synthesis of the Src SH2 binding peptide derived from the hmT antigen with sequence Ac-EPQpYEEIPIYL-NH<sub>2</sub> has been described previously.<sup>28</sup> This peptide is referred to as the pYEEI peptide. The Grb2 SH2 binding peptide Ac-PSpYVNVQN-NH<sub>2</sub> is derived from the Shc adaptor protein (position Y427 in hShc) and was synthesized as described.<sup>8</sup> This peptide is referred to as the pYVNV peptide. For coupling to the sensor matrix, these peptides were extended at the N-terminus with a 6-aminohexanoic acid (Ahx) moiety to provide a spatial linker between the sensor matrix and the phosphotyrosyl binding epitope, as described.<sup>8</sup>

The synthesis and characterization of the cyclic pYVNV construct (Chart 1) has been described previously.<sup>33</sup>

**SPR Binding Experiments.** SPR experiments were performed with an IBIS II instrument (Eco Chemie, Utrecht, The Netherlands), essentially as previously described.<sup>8</sup> In short, the Ahx-extended phosphotyrosyl peptides were covalently coupled to an SPR sensor chip through their free amino group using EDC/NHS chemistry. For the pYVNV peptide, a XanTec CMD20 SPR sensor disk was used (XanTec Bioanalytics GmbH, Munster, Germany). A concentration of 2 mM of the Ahx-pYVNV peptide in 0.1 M borate/1 M NaCl buffer pH 8.3 was reacted during 10 min. After repeated attempts, it appeared not to be possible to couple the Ahx-pYEEI-peptide

to the XanTec chip; therefore this peptide was coupled to a Biacore CM5 sensor chip (Biacore AB, Uppsala, Sweden). A concentration of 5 mM of the Ahx-pYEEI peptide in 0.1 M borate/1 M NaCl pH 8.3 was reacted during 10 min. Experiments were performed in Hepes-buffered saline pH 7.4 (HBS buffer) in a temperature range from 10 to 40 °C. The solutions were adjusted to temperature before injection to diminish temperature effects.

The binding constants of the proteins for the peptides coupled to the sensor ( $K_C$ ) as well as the maximum binding capacity were obtained from fitting the equilibrium SPR signal as a function of protein concentration with a one-site Langmuir binding isotherm.<sup>28</sup> In this assay, the free protein concentration was corrected for small depletion of protein due to binding.<sup>28</sup> Also, when the conformation change model applied (eq 2), the equilibrium signal could be excellently fitted with the one-site binding isotherm.<sup>8</sup>

The binding constant in solution ( $K_S$ ), defined as the thermodynamic binding constant for a bimolecular interaction, was obtained from SPR competition experiments.<sup>26</sup> The proteins in a fixed concentration (400 nM for both SH2 domains and 750 nM for full-length Grb2) were mixed with the phosphotyrosine peptides over a concentration range, and the SPR equilibrium signal was assayed.  $K_S$  was obtained from fitting the inhibition curve as described.<sup>26</sup>

**Thermodynamic Analysis of Binding Equilibrium and Transition State Formation.** The obtained affinity constants  $K_A$  (whether  $K_S$  or  $K_C$  (see above)) in a range from 10 to 40 °C were fitted with the integrated van't Hoff eq 3.

$$\ln K_A = \frac{-\Delta H^\circ(T^\circ)}{RT} + \frac{\Delta S^\circ(T^\circ)}{R} + \frac{\Delta C_p}{R} \left[ \left( \frac{T - T^\circ}{T} \right) - \ln \left( \frac{T}{T^\circ} \right) \right] \quad (3)$$

From this, the thermodynamic equilibrium parameters for binding,  $\Delta H^\circ$  and  $\Delta S^\circ$  at reference temperature  $T^\circ$  (25 °C), and the heat capacity  $\Delta C_p$  were derived.

According to transition state theory, kinetic data can be analyzed via the Eyring equation  $K^\ddagger = k\hbar/k_B T$ , in which  $K^\ddagger$  is the thermodynamic equilibrium constant for formation of the transition state,  $k$  is the on- or off-rate constant,  $\hbar$  is Planck's constant, and  $k_B$  is Boltzmann's constant. For linear Eyring plots, the activation parameters  $\Delta H^\ddagger$  and  $\Delta S^\ddagger$  are obtained from eq 4.

$$\ln \left( \frac{k_{\text{off}} \hbar}{k_B T} \right) = -\frac{\Delta H}{R} \frac{1}{T} + \frac{\Delta S}{R} \quad (4)$$

For the nonlinear Eyring plots,  $K^\ddagger$  in the form of the Eyring equation is treated in the same manner as for the equilibrium reaction and fitted with eq 3.<sup>45</sup> From this fit,  $\Delta H^\ddagger$  and  $\Delta S^\ddagger$  at the reference temperature (25 °C) and  $\Delta C_p^\ddagger$  are obtained.

**Assay of Off-Rates.** The off-rate constants ( $k_{\text{off}}$ ) of Src SH2 and full-length Grb2 protein have been assayed at temperatures in the range of 10 to 30 °C, essentially as described with some adaptations for measurement at various temperatures.<sup>8</sup> After equilibration of binding of 1  $\mu$ M protein at the desired temperature, agitation of the solution in the cuvette was stopped to obtain a stable signal, and 10  $\mu$ L of 1mM pYEEI or pYVNV peptide with adjusted temperature was rapidly manually added. The dissociation phase was assayed with a high sampling rate of five data points per second. The SPR signal is very sensitive to (small) temperature changes, and this was sometimes visible as a linear baseline with a small positive or negative slope within 10 s after addition of the peptide. The SPR signal in the dissociation phase ( $R(t)$ ) could be fit well to eq 5 with a monoexponential fit superposed on a baseline with slope  $b$  to correct for the above-mentioned temperature effect.

$$R(t) = a + bt + ce^{-k_{\text{off}}t} \quad (5)$$

For temperatures above 30 °C, no  $k_{\text{off}}$  values have been determined due to increased disturbance of the baseline. For these temperatures  $k_{\text{off}}$  was obtained by extrapolation from the

Arrhenius plot. The data points of the first second after addition of the peptide were discarded, as in this time interval the signal is strongly influenced by the bulk effect of mixing of the 1 mM peptide solution. At least three experiments at each temperature were performed to obtain  $k_{\text{off}}$ . The dissociation of Grb2 SH2 appeared to proceed extremely rapid and could not be accurately measured with this method.

**Global Kinetic Analysis of the SPR Signal.** Kinetic analysis of the association phase has been performed with the program CLAMP.<sup>11</sup> Global analyses were performed by fitting several curves from different protein concentrations simultaneously, using defined binding models (eqs 1 and 2). In the binding models, a mass transfer step from bulk solution to the sensor surface was included ( $k_{\text{tr}}$ ). In these fits, values for the maximum binding capacity and  $k_{\text{off}}$ , derived from independent experiments, have been introduced.

**Acknowledgment.** We thank Dr Isabel Catalina for MS characterization of the proteins.

## References

- Davis, A. M.; Teague, S. J.; Kleywegt, G. J. Application and limitations of X-ray crystallographic data in structure-based ligand and drug design. *Angew. Chem., Int. Ed.* **2003**, *42*, 2718–2736.
- Blundell, T. L.; Jhoti, H.; Abell, C. High-throughput crystallography for lead discovery in drug design. *Nat. Rev. Drug Discovery* **2002**, *1*, 45–54.
- Roberts, G. C. Applications of NMR in drug discovery. *Drug Discovery Today* **2000**, *5*, 230–240.
- Pellecchia, M.; Sem, D. S.; Wuthrich, K. NMR in drug discovery. *Nat. Rev. Drug Discovery* **2002**, *1*, 211–219.
- Weber, P. C.; Saleme, F. R. Applications of calorimetric methods to drug discovery and the study of protein interactions. *Curr. Opin. Struct. Biol.* **2003**, *13*, 115–121.
- Henriques, D. A.; Ladbury, J. E. Inhibitors to the Src SH2 domain: A lesson in structure–thermodynamic correlation in drug design. *Arch. Biochem. Biophys.* **2001**, *390*, 158–168.
- Glish, G. L.; Vachet, R. W. The basics of mass spectrometry in the twenty-first century. *Nat. Rev. Drug Discovery* **2003**, *2*, 140–150.
- De Mol, N. J.; Catalina, M. I.; Fischer, M. J. E.; Broutin, I.; Maier, C. S. et al. Changes in structural dynamics of the Grb2 adaptor protein upon binding of phosphotyrosine ligand to its SH2 domain. *Biochim. Biophys. Acta* **2004**, *1700*, 53–64.
- Cooper, M. A. Optical biosensors in drug discovery. *Nat. Rev. Drug Discovery* **2002**, *1*, 515–528.
- Markgren, P. O.; Lindgren, M. T.; Gertow, K.; Karlsson, R.; Hamalainen, M. et al. Determination of interaction kinetic constants for HIV-1 protease inhibitors using optical biosensor technology. *Anal. Biochem.* **2001**, *291*, 207–218.
- Morton, T. A.; Myszk, D. G. Kinetic analysis of macromolecular interactions using surface plasmon resonance biosensors. *Methods Enzymol.* **1998**, *295*, 268–294.
- Baerga-Ortiz, A.; Bergqvist, S.; Mandell, J. G.; Komives, E. A. Two different proteins that compete for binding to thrombin have opposite kinetic and thermodynamic profiles. *Protein Sci.* **2004**, *13*, 166–176.
- Day, Y. S.; Baird, C. L.; Rich, R. L.; Myszk, D. G. Direct comparison of binding equilibrium, thermodynamic, and rate constants determined by surface- and solution-based biophysical methods. *Protein Sci.* **2002**, *11*, 1017–1025.
- Songyang, Z.; Cantley, L. C. Recognition and specificity in protein tyrosine kinase-mediated signaling. *Trends Biochem. Sci.* **1995**, *20*, 470–475.
- Lim, W. A. The modular logic of signaling proteins: building allosteric switches from simple binding domains. *Curr. Opin. Struct. Biol.* **2002**, *12*, 61–68.
- Beattie, J. SH2 domain protein interaction and possibilities for pharmacological intervention. *Cell. Signalling* **1996**, *8*, 75–86.
- Sawyer, T. K. Src homology-2 domains: Structure, mechanisms, and drug discovery. *Biopolymers* **1998**, *47*, 243–261.
- Bradshaw, J. M.; Gruzca, R. A.; Ladbury, J. E.; Waksman, G. Probing the “two-pronged plug two-holed socket” model for the mechanism of binding of the Src SH2 domain to phosphotyrosyl peptides: A thermodynamic study. *Biochemistry* **1998**, *37*, 9083–9090.
- Waksman, G.; Shoelson, S. E.; Pant, N.; Cowburn, D.; Kuriyan, J. Binding of a high affinity phosphotyrosyl peptide to the Src SH2 domain: Crystal structures of the complexed and peptide-free forms. *Cell* **1993**, *72*, 779–790.
- Marengere, L. E.; Songyang, Z.; Gish, G. D.; Schaller, M. D.; Parsons, J. T. et al. SH2 domain specificity and activity modified by a single residue. *Nature* **1994**, *369*, 502–505.
- Rahuel, J.; Gay, B.; Erdmann, D.; Strauss, A.; Garcia-Echeverria, C. et al. Structural basis for specificity of Grb2-SH2 revealed by a novel ligand binding mode. *Nat. Struct. Biol.* **1996**, *3*, 586–589.
- Yuzawa, S.; Yokochi, M.; Hatanaka, H.; Ogura, K.; Kataoka, M. et al. Solution structure of Grb2 reveals extensive flexibility necessary for target recognition. *J. Mol. Biol.* **2001**, *306*, 527–537.
- Charifson, P. S.; Shewchuk, L. M.; Rocque, W.; Hummel, C. W.; Jordan, S. R. et al. Peptide ligands of pp60(c-src) SH2 domains: A thermodynamic and structural study. *Biochemistry* **1997**, *36*, 6283–6293.
- Chung, E.; Henriques, D.; Renzoni, D.; Zvelebil, M.; Bradshaw, J. M. et al. Mass spectrometric and thermodynamic studies reveal the role of water molecules in complexes formed between SH2 domains and tyrosyl phosphopeptides. *Structure* **1998**, *6*, 1141–1151.
- McNemar, C.; Snow, M. E.; Windsor, W. T.; Prongay, A.; Mui, P. et al. Thermodynamic and structural analysis of phosphotyrosine polypeptide binding to Grb2-SH2. *Biochemistry* **1997**, *36*, 10006–10014.
- de Mol, N. J.; Gillies, M. B.; Fischer, M. J. E. Experimental and calculated shift in  $pK_a$  upon binding of phosphotyrosine peptide to the SH2 domain of p56(lck). *Bioorg. Med. Chem.* **2002**, *10*, 1477–1482.
- Henriques, D. A.; Ladbury, J. E.; Jackson, R. M. Comparison of binding energies of SrcSH2-phosphotyrosyl peptides with structure-based prediction using surface area based empirical parametrization. *Protein Sci.* **2000**, *9*, 1975–1985.
- de Mol, N. J.; Plomp, E.; Fischer, M. J. E.; Ruijterbeek, R. Kinetic analysis of the mass transport limited interaction between the tyrosine kinase lck SH2 domain and a phosphorylated peptide studied by a new cuvette-based surface plasmon resonance instrument. *Anal. Biochem.* **2000**, *279*, 61–70.
- Schuck, P. Kinetics of ligand binding to receptor immobilized in a polymer matrix, as detected with an evanescent wave biosensor. I. A computer simulation of the influence of mass transport. *Biophys. J.* **1996**, *70*, 1230–1249.
- Faeder, J. R.; Hlavacek, W. S.; Reischl, I.; Blinov, M. L.; Metzger, H. et al. Investigation of early events in Fc epsilon RI-mediated signaling using a detailed mathematical model. *J. Immunol.* **2003**, *170*, 3769–3781.
- Felder, S.; Zhou, M.; Hu, P.; Urena, J.; Ullrich, A. et al. SH2 domains exhibit high-affinity binding to tyrosine-phosphorylated peptides yet also exhibit rapid dissociation and exchange. *Mol. Cell Biol.* **1993**, *13*, 1449–1455.
- Truhlar, D.; Kohen, A. Convex Arrhenius plots and their interpretation. *Proc. Natl. Acad. Sci. U.S.A.* **2001**, *98*, 848–851.
- Dekker, F. J.; de Mol, N. J.; Fischer, M. J. E.; Kemmink, J.; Liskamp, R. M. Cyclic phosphopeptides for interference with Grb2 SH2 domain signal transduction prepared by ring-closing metathesis and phosphorylation. *Org. Biomol. Chem.* **2003**, *1*, 3297–3303.
- Chook, Y. M.; Gish, G. D.; Kay, C. M.; Pai, E. F.; Pawson, T. The Grb2–mSos1 complex binds phosphopeptides with higher affinity than Grb2. *J. Biol. Chem.* **1996**, *271*, 30472–30478.
- Anderegg, R.; Wagner, D. Mass spectrometric characterization of a protein–ligand interaction. *J. Am. Chem. Soc.* **1995**, *117*, 1374–1377.
- Nioche, P.; Liu, W. Q.; Broutin, I.; Charbonnier, F.; Latreille, M. T. et al. Crystal structures of the SH2 domain of Grb2: highlight on the binding of a new high-affinity inhibitor. *J. Mol. Biol.* **2002**, *315*, 1167–1177.
- Baker, B. M.; Murphy, K. P. Prediction of binding energetics from structure using empirical parametrization. *Methods Enzymol.* **1998**, *295*, 294–315.
- Holdgate, G. A.; Tunnicliffe, A.; Ward, W. H.; Weston, S. A.; Rosenbrock, G. et al. The entropic penalty of ordered water accounts for weaker binding of the antibiotic novobiocin to a resistant mutant of DNA gyrase: A thermodynamic and crystallographic study. *Biochemistry* **1997**, *36*, 9663–9673.
- Maignan, S.; Guilloteau, J. P.; Fromage, N.; Arnoux, B.; Beccart, J. et al. Crystal structure of the mammalian Grb2 adaptor. *Science* **1995**, *268*, 291–293.
- Etmayer, P.; France, D.; Gounarides, J.; Jarosinski, M.; Martin, M. S. et al. Structural and conformational requirements for high-affinity binding to the SH2 domain of Grb2(1). *J. Med. Chem.* **1999**, *42*, 971–980.
- Wei, C. Q.; Gao, Y.; Lee, K.; Guo, R.; Li, B. et al. Macrocyclization in the design of Grb2 SH2 domain-binding ligands exhibiting high potency in whole-cell systems. *J. Med. Chem.* **2003**, *46*, 244–254.
- Garcia-Echeverria, C.; Furet, P.; Gay, B.; Fretz, H.; Rahuel, J. et al. Potent antagonists of the SH2 domain of Grb2: optimization of the X+1 position of 3-amino-Z-Tyr(PO<sub>3</sub>H<sub>2</sub>)-X+1-Asn-NH<sub>2</sub>. *J. Med. Chem.* **1998**, *41*, 1741–1744.

- (43) Cooper, A. Thermodynamic analysis of biomolecular interactions. *Curr. Opin. Chem. Biol.* **1999**, 3, 557–563.
- (44) Guilloteau, J. P.; Fromage, N.; Ries-Kautt, M.; Reboul, S.; Bocquet, D. et al. Purification, stabilization, and crystallization of a modular protein: Grb2. *Proteins* **1996**, 25, 112–119.
- (45) Chen, B. L.; Baase, W. A.; Schellman, J. A. Low-temperature unfolding of a mutant of phage T4 lysozyme. 2. Kinetic investigations. *Biochemistry* **1989**, 28, 691–699.

JM049359E